HAZ MICROSTRUCTURE AND PROPERTIES OF PIPELINE STEELS

R.C. Cochrane

Consultant, Visiting Research Professor, University of Leeds
Formerly British Steel Professor of Ferrous Metallurgy, University of Leeds

Abstract

The weld heat affected zone (HAZ) in steels differs appreciably in both microstructure and properties from the parent steel as a consequence of the thermal cycles involved in either pipe manufacture or during the laying of transmission pipelines. In the former case, two pass welding is often used in producing the individual lengths of pipe which constitute the pipeline; firstly a pass is made filling the inside joint, then a final pass sealing the outer pipe surface. The thermal cycles surrounding such welds are determined by the welding heat input used and will vary with plate thickness. Examples of the range of microstructures encountered for typical pipe plate compositions are reviewed and their influence on the mechanical properties of the seam weld assessed. There are several regions of the HAZ where significant changes in properties may be encountered. The first of these is the coarse grained HAZ (CGHAZ), the focus of this paper, secondly in the intercritical (IC) or grain refined (GR) regions of the HAZ and, thirdly, those regions where the CGHAZ microstructure of the first welding pass is modified by the subsequent weld run on the outside surface. The latter causes tempering of the original CGHAZ structure, whilst there may be additional embrittlement from precipitation or other microstructural changes. The factors leading to the evolution of the CGHAZ microstructure during cooling after welding are, primarily, the austenite grain size resulting from the weld heating cycle and the steel composition. The major microstructural changes are the formation of martensite or mixtures of martensite/bainite and these depend, critically, on the transformation behaviour of the steel. As carbon contents have been reduced over the past 3 decades, increasingly, 'carbide free' bainitic microstructures have become a feature of the CGHAZ and some consideration is given to the prospects for developing acicular ferrite HAZ microstructures. The poorer properties associated with the IC and GRHAZ remain and may be exaggerated by higher alloy content used to depress transformation temperature in more recent pipe steel compositions. The role of microalloying in controlling the grain coarsening response is assessed in the light of the size and distribution of the microalloy precipitates in the parent plate. These considerations lead to the conclusion that a significant part of the microstructural changes, including changes in precipitate response to the thermal cycle, in various regions of the HAZ are indirectly linked to the process history of the parent steel. Examples are described for some simple steels.

Introduction

Steels for pipeline construction range from the simple, based on C-Mn compositions, typically used for water transmission at low pressures, to the complex, carefully engineered and processed compositions used for oil or gas transmission in sub-sea or harsh environments, for example the Arctic. The latter steels are characterised by sophisticated chemical compositions, usually microalloyed with combinations of Nb, V and/or Ti, allied with precise control of their processing. The most desirable attribute of a steel is that the mechanical properties across the welded region remain as uniform as possible, ideally matching those of the parent steel and at the most economic cost, 'the metallurgist's delight'. In other words, the ease of weldability is paramount.

In the context of pipeline construction, there are 2 aspects of weldability that need to be considered: firstly, the influence of the welding process used in the pipe-making operation and secondly, the effects of welding pipe lengths to form the finished pipeline. In the latter case, some consideration might also need to be given to joining of 'crack arrester' components, should these be part of the pipeline design. The metallurgical changes resulting from welding during pipe production are, largely, the result of the effect of the thermal cycle resulting from the passage of a molten weld pool through the steel. In the case of seam welding of linepipe, the extent of the HAZ, and the corresponding changes in mechanical properties, depend on the plate thickness and the weld heat input, usually in the ranges ~8 to around 45 mm and <~3 to >~10 kJ/mm respectively, with the lower end of this range being more typical of spiral welded pipe, where pipe wall thicknesses are generally lower, up to ~25 mm.

Pipe to pipe joining, to form the transmission line, is generally designed to match as closely as possible (if not overmatch) the original pipe properties and, in achieving this, the weld design is such that many small passes are used and a correspondingly narrow HAZ results. In general terms, the extent of the mechanical property changes is modest and rarely a major problem, apart from a need imposed by specification to limit the weld zone hardness to some particular value, and where the hydrogen originating from the welding process may lead to hydrogen induced cold cracking (HICC) in either the HAZ or the weld metal.

This paper concentrates on the microstructural changes, and hence, mechanical properties caused by the thermal cycles attendant on 2-pass seam welding of linepipe. Firstly, a brief review of the effects of weld thermal cycles will be presented as an introduction to surveying the microstructural changes in particular regions of the HAZ and how these are related to various aspects of the steel composition. In doing so the effects of the metallurgical processing used for pipe plate production on the nature and distribution of the microalloying precipitates will be highlighted.

Metallurgical Effects of Welding

Heat Flow

It is convenient to regard the weld thermal cycles, and therefore the metallurgical changes, as a simple function of three variables: thickness of the material being welded, the initial temperature of the material and the amount of energy input from the welding operation. This latter quantity is termed heat input, expressed as energy per unit length of weld. A nearly exact solution of the heat flow around a weld was first proposed by Rosenthal [1] and formed the basis for most of the subsequent modelling of the HAZ thermal profile. A typical analytical expression for the heat flow during welding is shown in Figure 1 from the work by Nippon Steel Corporation [2]. Such mathematical models allow an almost complete description of the time temperature profiles around a weld. In most cases a simplifying approximation is made that the weld is a point source of heat; however, some error is introduced by this assumption and recent modelling has included the case where the weld pool length is not negligible as in multiple wire seam welding of pipe [3]. For the steel compositions used in pipe production, the transformation from austenite formed in the HAZ takes place largely over the temperature range 800 to 500 ^{o}C. The time taken to cool between these temperatures, $\Delta t_{800/500}$, is related to the weld heat input and the other variables mentioned above. Various nomograms exist for predicting an appropriate value for cooling time, an example is shown in Figure 2, although care is needed in their use.
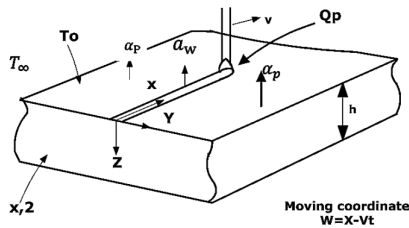
$$T = T_\infty + \frac{Q_p}{\pi\lambda h}\exp\left(-\frac{vw}{2x}\right)\Sigma_{n=0}^{\infty} A_{wn}\left(\cos\frac{u_{wn}Z}{h} + \frac{hd_w}{U_{wn}}\sin\frac{u_{wn}Z}{h}\right)X$$

$$K_o\left(\frac{r}{h}\sqrt{u_{wn^2}(\frac{vh}{2x})}2\right) + 2(T_\circ - T_\infty)\overset{\infty}{\underset{n=0}{\Sigma}}A_{Pn}\left(\cos\frac{u_{Pn}Z}{h} + \frac{hd}{u_{Pn}}\sin\frac{u_{Pn}Z}{h}\right)X$$

$$\left\{\frac{\sin u_{Pn}}{u_{Pn}} - \frac{hd_p(\cos u_{Pn} - 1)}{U_{Pn}2}\right\}\exp\left(-\frac{u_{Pn}2}{h^2}t\right)$$

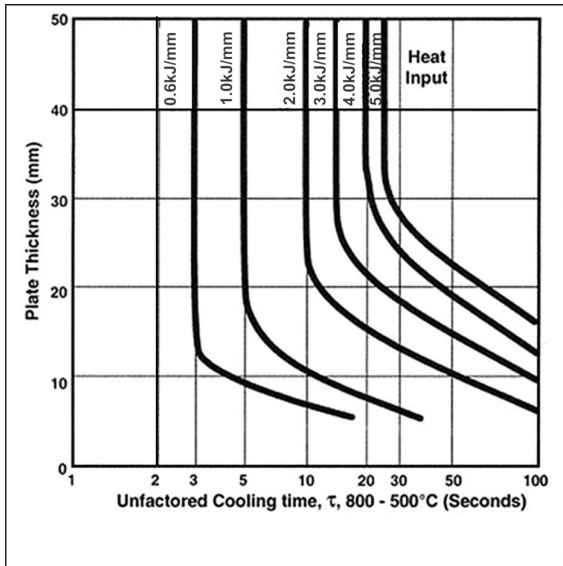Figure 1. The general form of the weld heat flow equation, after [2].

Figure 2. A nomogram for estimating the cooling time at the fusion line of a weld HAZ.

While the weld thermal cycles at various distances from the fusion boundary can now be modelled rather precisely, from a metallurgical point of view they broadly divide into the following regions (the width of which depends somewhat on the transformation characteristics of the steel, but always increases with weld heat input, alternatively, the characteristic weld HAZ cooling time, $\Delta t_{800/500}$):

SCHAZ, Sub-Critically Reheated HAZ. This is a region where the steel is heated to some temperature below the lower critical temperature or Ac1 of the steel. Little or no change in microstructure occurs in this region, but it should be remembered that microalloyed steels rely on precipitation and some additional precipitation or over-ageing effects may occur in this region, particularly when high heat inputs, >about 3-5 kJ/mm, are used. Any metallurgical effects are usually assumed negligible below 450 to 500 $^{\circ}$C.

ICHAZ, Inter-Critically Reheated HAZ. In this region the steel is heated to temperatures between the Ac1 and Ac3 points where a microstructure of ferrite and austenite is produced at the peak temperature reached during the weld cycle. The microstructure across this region therefore depends on the peak temperature reached and the subsequent cooling time and therefore a wide range of microstructures are formed. If the cooling time is rapid and the peak temperature is close to the Ac1, hard brittle martensite with a high carbon content will be

156

formed, conversely if the peak temperature is close to the Ac3 the martensite volume fraction will be larger and the carbon content lower. Note that transformation to high carbon martensite occurs below ~300 $^{\circ}$C.

GRHAZ, Grain-Refined HAZ. In this region the steel is heated into the austenite phase field but little or no grain growth occurs, the resulting austenite grain size is therefore fine and ferrite re-forms on cooling from the peak temperature. Across this region the peak temperature reached lies between the Ac3 and, for microalloyed steels, the solvus of the precipitating species. Depending on the cooling rate, martensite may also be present as in the ICHAZ.

CG or GCHAZ, Coarse Grained or Grain Coarsened HAZ. This region of the HAZ is where austenite grain growth is extensive because of the peak temperatures reached; in microalloyed steels the characteristic temperature above which this region becomes pronounced is usually above the solvus for the microalloying addition(s) used in the steel. The width of this region dominates the impact behaviour of welds. There are 2 principal effects on mechanical properties, one arises from the change in microstructure and the other relates to the dissolution of microalloy precipitates.

In 2 pass welds characteristic of pipe seam welding, there are other regions of the HAZ which experience thermal cycles as the HAZ formed by the inside pass is reheated by the outer bead pass. The two most significant, in terms of changes in mechanical properties or ability to meet pipe specifications, are:

ICCGHAZ, Intercritically Reheated Coarse Grained HAZ. This is a region in which the coarse austenite structure first transforms to a coarse bainitic or martensitic microstructure which is subsequently reheated into the austenite/ferrite phase field forming a coarsened bainitic structure with embedded regions of high C austenite which transforms to a range of microstructures during cooling from the peak interpass temperature. These are commonly referred to as 'microphases' or retained austenite and martensite constituents, M/A phase will be used in the remainder of the paper.

SCCGHAZ, Sub-Critically Reheated Coarse Grained HAZ. This region is generally not important in C-Mn steels although tempering of brittle constituents will occur which tends to be beneficial to toughness. However, in microalloyed steels additional precipitation can occur on reheating the CGHAZ producing additional embrittlement.

The location of these zones relative to the weld is shown in Figure 3a and the corresponding thermal cycles in Figure 3b. Note however, whilst thermal cycles can be modelled and, with a degree of difficulty measured, the austenitising response of the steel is often assumed to be relatively constant.

The 'Sampling' Problem in HAZ Mechanical Properties

In general, it is difficult to identify uniquely systematic effects of composition, particularly those due to microalloying, on HAZ mechanical properties because of large variations in individual Charpy values taken from nominally identical positions. Part of the scatter can be understood in

terms of the positioning of the Charpy notch in the HAZ, Figure 4, which, in most pipe welds, samples a range of microstructures. Bearing in mind that seam weld bead width and depth can vary along the welded length, a nominal fusion line, FL, location can vary by a minimum of +/- 0.5 mm from this nominal position leading to a 'natural' scatter in results due to the severe microstructural gradient away from the fused zone. To mitigate the 'sampling' problem, HAZ testing is usually specified with respect to a nominal fusion line (FL) position plus some distance marker, for example FL, FL +1 mm, FL +3 mm etc., Figure 4. A judgement must then be made as to the deterioration of HAZ properties by comparing sets of data from different pipes for a particular application. To place these effects in context it is worthwhile remembering that for a typical pipe weld HAZ the CGHAZ may only comprise 10 to 20% (1 to 2 mm) of a Charpy notch placed at the fusion line position and given the tolerances involved in location a wide scatter in results is inevitable. In addition, the measured Charpy energy values will be greatly influenced by weld metal toughness. With some pipe weld thickness, and bead geometries, the notch location may include regions of the ICCGHAZ or SCCGHAZ formed when the outer weld bead reheats the CGHAZ regions which formed during deposition of the inner bead. Should this region be suspected of being critical in terms of properties, it is almost impossible to judge without further testing, for example CTOD, whether this region of the HAZ is responsible for poor toughness, partly because of the limited size of these zones. Hence in some cases additional criteria, such as a limitation on weld zone hardness, are included in some pipe specifications. CTOD (crack tip opening displacement) testing has, also, been commonly used, and occasionally required by specification, to sample embrittled regions, so-called local brittle zones, because the fatigue crack tip is much sharper and therefore more easily placed in that particular region, as in Figure 4. Such tests are known to be influenced by local residual stresses around the weld, and for pipe welds these are influenced by pipe expansion strains.
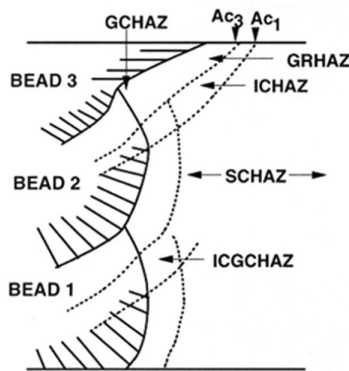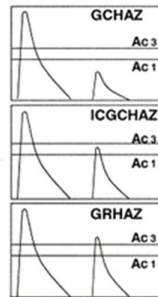

Fig. 3a   Fig. 3b

Figure 3. Schematic showing the various regions of microstructural change around a weld, although this shows 3 beads the thermal cycles remain unchanged.
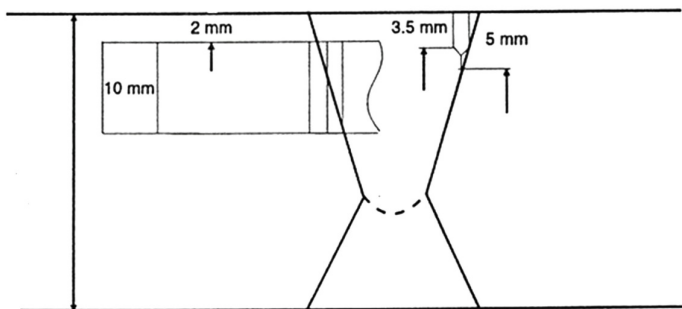
Figure 4. Showing typical locations for Charpy test pieces and notch positioning for CTOD tests for CGHAZ toughness.

By generating weld bead profiles which result in gently sloping fusion boundaries, as in Figure 5, the general form of the changes in Charpy or CTOD properties across the HAZ is more easily observed. This technique has the advantage that the HAZ is comparable to that of a pipe weld in terms of width and microstructural gradient with notch placement being rather easier although still subject to similar scatter. A variant of this uses a weld preparation with a straight edge along which the notch is placed. In either case, the effects of steel composition can be examined in terms of microstructural changes and effects on mechanical properties. The effect of $\Delta t_{800/500}$ on microstructure is also easily assessed by changing heat input or preheat temperature.
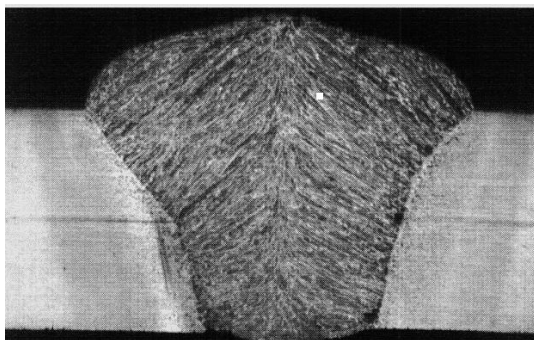

Figure 5. Typical weld bead profile for HAZ toughness assessment at high heat inputs, this example is 7.5 kJ/mm.

159

A more useful technique, and in reality the only way of comparing the effects of particular additions on HAZ tensile properties, is that of HAZ simulation. Here the steel is subjected to thermal cycles derived from the various mathematical models of welding although it can be difficult to achieve the heating rate comparable to that of a weld. The great advantage is that a large volume of simulated weld HAZ microstructure is available for study and the effects of the thermal cycles resulting from additional welding passes can be examined in detail (by reproducing the relevant thermal cycles) unlike the small volumes available from 'real' welds. However, the significance of the thermal gradient implicit in a 'real' weld should not be underestimated. During HAZ simulation, austenite grain growth is essentially unrestrained unlike that in a weld where austenite grains formed at lower temperatures, and therefore smaller, have a marked effect on the size to which the CGHAZ austenite grains grow since this region may be, at most, only a few grains wide depending on the grain growth behaviour of the steel and heat inputs involved in seam welding. At the other extreme, the absence of the liquidus adjacent to the weld pool also changes grain growth characteristics during simulation. Nevertheless, results from simulation can provide microstructural information germane to optimisation of steel composition.

Generic Effects of Steel Composition and Processing on HAZ Mechanical Properties

A 'carbon equivalent value' (CEV), of which there are many, can be calculated for any steel composition and applied to judge potential weldability: the most commonly used are Lloyds or P_{cm} formulae as used by Graville [4], Figure 6. Much more reliance is placed on empirical correlations between composition, toughness and/or hardness and there are many such empirical relationships described in the literature relating HAZ properties, usually hardness or impact toughness to composition, an early example is shown in Figure 7 [5]. Whilst many such correlations, such as the IIW CEV or the various alternative formulae have been presented, most assume some typical austenite grain size which is known to be sensitive to alloy content or steel composition and thermal cycle [6-10]. Much less is known, and not well documented, about the influence of process route. In this context, the differences in grain growth behaviour between modern steels of increasing cleanness or residual levels and steels of an earlier generation can be marked and lead to situations where empirical rules derived on the basis of the latter group of steel no longer hold true. It is worth pointing out here that some of the empirical relationships, from which restrictions on composition in pipe specifications are often generated, are based on steels first developed some 40 years ago. With the continuing improvements in steelmaking and processing technologies, some of these might usefully be revised. Such a situation will continue to arise as steelmaking techniques improve or processing changes.
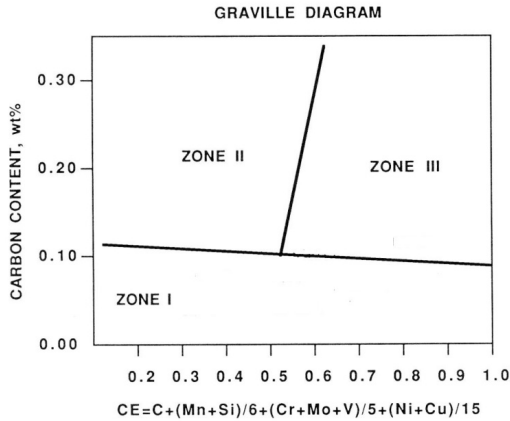
GRAVILLE DIAGRAM

Figure 6. Diagram due to Graville [4] intended to indicate the ease of Weldability, Zone 1 being where little care is needed, Zone II some care and Zone III considerable care is necessary.
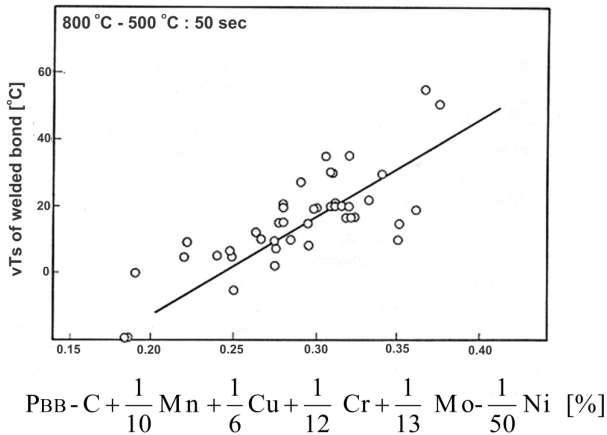

$$P_{BB} - C + \frac{1}{10} Mn + \frac{1}{6} Cu + \frac{1}{12} Cr + \frac{1}{13} Mo - \frac{1}{50} Ni \ [\%]$$

Figure 7. Example of correlation between steel composition and CGHAZ Charpy transition temperature. Adapted from [5], P_{BB} is a measure of the weld bond brittleness.

By correlating the performance in service or study of mechanical testing of welds at FL, FL+1 etc., with one or other of the CEV formula (such as P_{cm} [10] or P_{BB} [5], Figure 7) some limit, generally derived from service performance criteria, can be placed on steel composition. Hence,

for example, a hardness limitation of, say, 350 Hv may imply a maximum CEV of, say 0.38 but this restriction takes little or no account of the other factors implicit in controlling transformation behaviour, such as HAZ cooling rate or austenite grain size. Some of the carbon equivalent formulae specifically contain factors for microalloying additions [6,7] and $\Delta t_{800/500}$ [6-10]. Few include a measure of the influence of austenite grain size widely regarded as a key parameter in establishing the range of microstructures or hardenability as would be the case for conventional heat treatment. As an example, for a typical X65 composition (0.09%C 1.45%Mn 0.03%Nb 0.3%Cu+Ni) the cooling time to form a 90% martensite/bainite microstructure can change from 8.5 (35 ^{o}C/sec) to 12 (25 ^{o}C/sec) seconds if the austenite grain size changes from 100 to 150 μm, accompanied by a significant change in hardness [11]. The cooling time change is equivalent to a not inconceivable deviation in heat input from 1.6 to 2.0 kJ/mm for a 20 mm plate thickness [2] emphasising the need for precise control of welding parameters during seam welding. In addition, some particular microstructures arising during weld thermal cycles, such as bainite, acicular ferrite or martensite or mixtures thereof, are associated with particular ranges of toughness and hence the transformation characteristics invariably dictate the level of toughness observed.

That the HAZ microstructure is determined by the transformation characteristics of the steel from an austenite grain size characteristic of the HAZ thermal cycle in question, is self evident. Therefore, development of austenite grain size during the thermal cycle, particularly in the presence of microalloying elements, is closely linked to the deterioration of properties after welding, even at constant composition, and is dealt with in a later section.

Generic Changes in Toughness or Hardness Across the Weld HAZ

That there is always deterioration in weld HAZ properties seems to be a common myth among welding engineers and metallurgists. Such attitudes probably arose due to the types of steel available at the dawning of welding technology. Given that steels of that era were appreciably higher carbon content than those currently used, coupled with the use of generally lower weld heat inputs then a high hardness after welding was inevitable. The austenite grain growth behaviour of these steels, most of which were not 'microalloyed', differed from those currently in use and relied on Al and/or Si for deoxidation. Take the example, not untypical of 75 years ago, of a normalised 0.2%C plate steel, the martensitic hardness could be in excess of 350 Hv in the HAZ and the impact toughness would be significantly inferior to the softer ferrite/pearlite parent plate microstructure. As microalloyed steel technology developed the link between C content and mechanical properties altered because the necessary ferrite grain size refinement could be produced by controlling the austenite grain size by dispersions of either AlN and/or NbC or VN. Consequently, not only could carbon content be reduced but the parent steel properties increasingly depended on conditioning of the austenite allowing independent control of the ferrite grain size and the extent of precipitation strengthening from the microalloying additions.

It is therefore quite instructive to consider the relative changes in HAZ properties for a simple microalloyed steel where the parent plate strength is similar but the impact properties differ considerably. These differences in properties can be achieved by controlling the rolling of a simple C-Mn-Nb (0.14%C 1.35%Mn 0.036%Nb) to very different rolling schedules, in this case on a reversing plate mill. One is dictated by the need to maximise plate mill throughput, termed

as-rolled, AR, the other designed to optimise plate properties by control of rolling operations, now better known as thermomechanical controlled rolling, TMCR. If such steels are welded with bead profiles as shown in Figure 5 then the changes in toughness across the HAZ can be examined. Although the schedules were designed to achieve similar yield strength, say 350 - 420 MPa, the absolute values of Impact Transition Temperature (ITT) differed, in the range -10 to 20 ^{o}C for AR compared to -20 to -50 ^{o}C for the TMCR steel. The pattern of relative (note, not absolute values) changes in HAZ toughness is shown in Figure 8. Note that in the AR steel the CGHAZ properties improve marginally after welding compared to the dramatic fall for the TMCP condition. This situation arises because of the nature of the structure/property relationships for the different rolling conditions. In the AR condition, the impact toughness of the base steel is a balance between the improvement from refining ferrite grain size, $\sim$-10 ^{o}C/d$^{-1/2}$ (mm$^{-1/2}$), and the deterioration by precipitation hardening, σ_p, +0.5 ^{o}C/MPa,. In the TMCR case, a similar range of yield strengths matching those in the AR condition, can be achieved almost entirely by ferrite grain refinement alone which greatly improved the impact toughness of the base steel. Put in simplistic terms, since the CGHAZ microstructure is largely a function of the welding cycle in both cases, by processing the same steel composition in different ways weldability has changed, in that in the AR condition there is little deterioration, to the metallurgist, a delight; after TMCP processing there is a dramatic change, to the welding engineer, a nightmare? However, if CGHAZ hardness is the sole arbiter of weldability then there is little difference as this is determined largely by the steel composition.
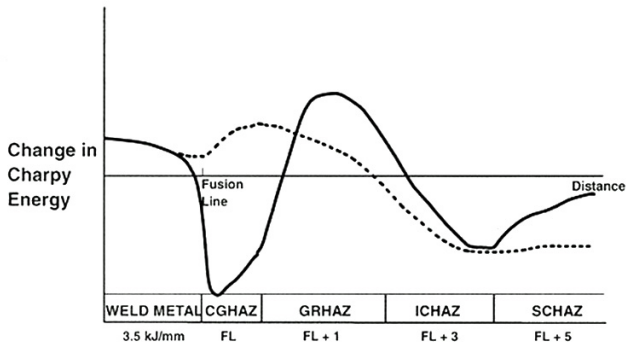

Figure 8. General trends in relative Charpy energy as a function of distance from the fusion line. The dotted line refers to AR steel, solid line is for TMCR steel and the horizontal line represents the relative (not absolute) base toughness of the parent steels.

The contrast depicted for this particular steel, between the conventionally processed and TMCR conditions serves to make a point, but it must be remembered that the changes are relative to different baselines, with that of the TMCR steel being considerably higher. Also it should not be assumed to be the same for other steel analyses, processing routes or welding procedures. More

particularly, this comparison can only be taken to imply that TMCR steels show comparatively larger changes as a consequence of their particular process route and do not suggest such steels are inferior in service because there is vast experience elsewhere which confirms that this is not the case. The results included herein are simply presented to illustrate the possibility that processing history and other factors may have to be taken into account when evaluating the weldability of HSLA steels.

For the AR steel, the minimum toughness does not correspond to the CGHAZ but in common with TMCP this lies in the ICHAZ, in this case corresponding to the formation of a relatively fine grained ferrite contained high carbon brittle martensite. Although AR steels are rarely used for premium pipe plate, these differences serve to illustrate the effects of parent plate microstructure on one aspect or other of the toughness across the whole of the HAZ. Of course, because of the 'sampling' problem discussed earlier, whether such differences show up in routine specification testing is debatable. Nevertheless, these effects illustrate coupling between ferrite grain refinement and precipitation hardening used to develop the base plate mechanical properties and the overall changes in HAZ properties for a given thermal cycle.

Microstructural Aspects of the ICHAZ and GRHAZ

In general terms, the ferrite grain size of the IC or GRHAZ is governed by the kinetics of re-austenitisation. Re-austenitisation begins at pearlite colonies but at rapid heating rates, as in the weld HAZ, also at ferrite/ferrite boundaries [for example, 12]. Consequently, it has been shown that the final austenite grain size reached is largely controlled by the initial or parent plate ferrite grain size and there are direct relationships between ferrite grain size and austenite grain size in various types of steel [13,14]. In the ICHAZ the austenitising process is only partially complete before cooling takes place, thus the microstructure largely reflects the parent plate ferrite grain size and the peak temperature reached. For a given ICHAZ weld cycle, changes in properties will be closely related to those of the parent plate.

Hence, for example, if the toughness of a C-Mn AR steel is comparatively poor and results from the formation of a coarse ferrite grain structure, say 10 to 15 microns, then, in the absence of microalloying additions, the corresponding GRHAZ grain size can be somewhat smaller, say 7 to 9 microns. Equally, should the precipitation contribution to strength be high, as in as-rolled C-Mn-Nb steels, and, as little coarsening occurs during the GRHAZ cycle, the particles remain ineffective at pinning the austenite grain structure. The resulting GRHAZ ferrite will then be on a scale similar to that of the parent ferrite structure. Where microalloy particles are relatively coarse, as after TMCR, some 10s of nanometres, despite some coarsening from the weld cycle, they remain effective in resisting austenite grain growth. In such cases the GRHAZ ferrite grain size may be close to that of the parent steel, typically, for TMCP X60 to X70 grades around 4 to 8 microns.

These microstructural changes might imply relatively good toughness, provided the cooling rate in the GRHAZ is slow enough to allow pearlite to re-form in the high carbon austenite remaining at the end of ferrite transformation. However, this is only likely at cooling rates slower than about 1 - 5 ^{o}C/sec, corresponding to $\Delta t_{800/500}$ values associated with comparatively large weld heat inputs and/or high preheat and/or interpass temperatures, depending on plate thickness. Consequently, in most seam welded pipe, the austenite will transform to either bainitic or martensitic microstructures of near eutectoid composition. Unless there is retained austenite, and

this depends on other alloy elements being present (the key ones being, Ni, Si, Mn and Mo in order of effectiveness), a hard brittle constituent will be present and the beneficial effects of the ferrite grain size on toughness will be partially lost.

The effects of V or Nb/V additions on GR or ICHAZ microstructure can be complicated by post weld cooling rate. The solvus temperature of V compounds is lower than that of Nb and as the optimum precipitation hardening response for V treated steels lies in the range 1 to 10 °C/sec significant additional embrittlement from precipitation may take place during cooling after welding. Although vanadium can sometimes produce a favourable microstructure in the CGHAZ with increased fracture energy absorption, see later, GRHAZ toughness can be dramatically reduced by precipitation for some combinations of plate thickness and heat input.

<u>CGHAZ Toughness, Microstructure and Steel Composition</u>

Results from near parallel sided high heat input single pass welds, in this case ~10 kJ/mm as shown in Figure 9 illustrate the beneficial effects of reducing CEV on the CGHAZ impact properties of TMCR steels.
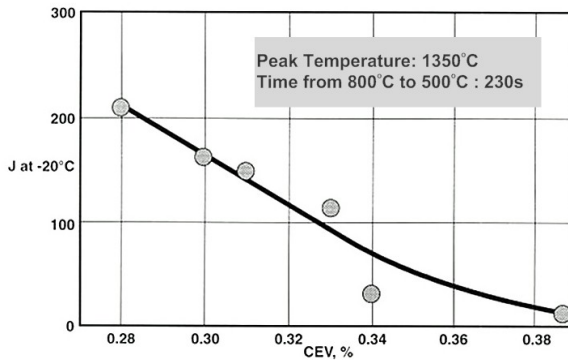

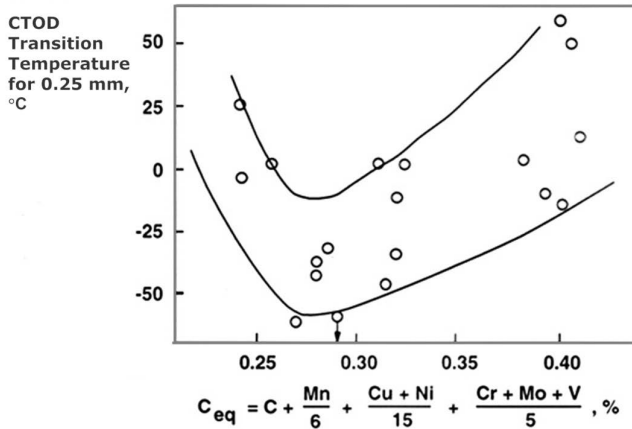Figure 9. Effect of CEV (Lloyds formula) on energy absorbed at -20 °C.
C-Mn-Nb steels.

Figure 10. Effect of CEV on CGHAZ CTOD transition temperature for TMCR steels welded at 5 kJ/mm. Adapted from Nakanishi et al [15].

In contrast, the effects of CEV on the CGHAZ CTOD transition temperatures of similar steels [15] albeit at lower heat input ~5 kJ/mm, appear to show a minimum around 0.28 to 0.30, Figure 10. Of course, had a wider range of CEV been included, below 0.28, in Figure 9 then it is possible that an optimum value would have been deduced as with the CTOD around 0.28 - 0.3 CEV for the particular steel compositions studied. In practice, CEV values for TMCR steels below ~0.28 - 0.3 would not have met the steel strength specification required in this case. However, Figures 9 and 10 should not be assumed to imply that a further reduction in CEV will not be beneficial in certain steel types or with process routes other than thermomechanical rolling.

For a fixed cooling time, the trend in Charpy toughness can be understood in terms of the hardenability of the steels. A fairly simple way of predicting hardenability was proposed by Maynier [16] who generated equations allowing hardness to be predicted from steel composition and a parameter which is a measure of austenite grain size, which, as already alluded to, is critically important. A further set of equations can then be used to predict a cooling rate (or $\Delta t_{800/500}$) to form a fully martensitic, bainitic or pearlitic microstructure. Although these equations strictly apply to heat treated steels, they can be, with caution, applied to HAZ 'heat treatment'. An alternative approach can be based on study of relevant CCT diagrams for the steels in question and the change in transformation behaviour assessed for a range of austenite grain size. However, such an approach is not entirely appropriate for microalloyed steel because to alter austenite grain size by peak temperature alone changes the microalloy solubility. Which ever method is used, it is clear that, for a given austenite grain size, lowering C content reduces the cooling time (raises cooling rate) required to form a fully martensitic structure meaning that modern low carbon steels generally have a mixed martensite/bainite CGHAZ microstructure with a lower hardness. Conversely, adding substitutional alloying elements can increase the

critical cooling time to form a fully martensitic structure. Several such models now exist based on this methodology and some are coupled to a model for austenite grain growth to provide predictions of CGHAZ microstructure [e.g 17-19] but few consider the effects of inhomogeneous solute (substitutional mainly but also C) distribution resulting from rapid heating [e.g. 18].

From the large number of studies of HAZ toughness, involving both 'real' welds, modelling and simulation, some general conclusions can be arrived at regarding the relative ranking of the different types of microstructures formed in the HAZ thermal cycles. These are summarized in Figure 11 adapted from work by Kirkwood and others [20-22] on TMCP steels with compositions similar to those used for pipe plate.
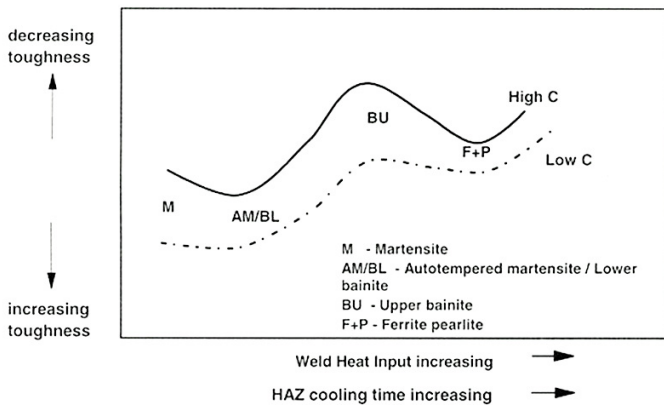

Figure 11. Schematic diagram of the effect of microstructure, C content and heat input on toughness, after Kirkwood [20].

Broadly, this indicates that low C steels will perform better than higher C steels and a fully martensitic microstructure is more beneficial than that termed bainitic in line with the general observations presented earlier. That this is not a complete picture, can be seen from Figure 12 which indicates, schematically, the path taken by cracks as they traverse different microstructures.
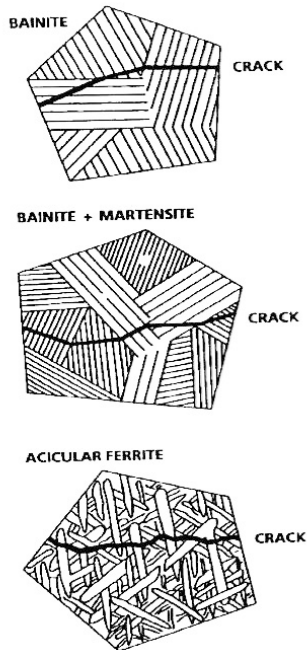
Figure 12. Diagrammatic representation of crack propagation in different microstructures, martensitic structures differ from bainite in terms of lath size and carbide distribution.

Bainitic and martensitic microstructures are characterised by groups of laths transforming from the parent austenite with different variants of the austenite/bainite-martensite crystallographic orientation relationships within a single austenite grain, each group forming a 'colony'. The colony size controls the crack path since cracks are deflected at the colony boundaries, consequently, energy is absorbed and toughness increased. However, the thicker filamentary carbides characteristic of upper (or type I) bainite at inter-lath boundaries are more embrittling than either the fine autotempered carbides characteristic of a fully martensitic structure or the fine carbides at lath edges in lower bainite (type II or type III). Hence, there is an overwhelming effect of transformation characterisitics where upper bainite structures predominate. This can be offset in the particular case of mixed martensitic and bainitic microstructures where the colony size is smaller than for either phase alone signifying improved toughness. Accordingly, there will be a primary effect of austenite grain size on toughness via the colony size and several studies have shown a correlation between colony size and fracture facet size measured in toughness tests. Some studies have confirmed a Hall-Petch type relationship and the effect of fracture facet size is similar to that of ferrite grain size in ferrite-pearlite steels, values in the literature range from -10 to 25 ^{o}C/mm$^{-1/2}$ [23, 24]. Assuming the colony size is proportional to austenite grain size, a finer grained CGHAZ would be expected to show improved toughness. However, others

claim that lath size and/or lath misorientation are equally important [25, 26] since some energy is absorbed traversing interlath boundaries. As lath dimensions are a function of carbon content, then the coarser lath sizes in low C steels might imply some loss of toughness but this is compensated by the increase in transformation temperature which lowers the dislocation content as well as increasing lath dimensions [27]. These general trends in microstructure are in agreement with the pattern of results in Figure 11.

With the much lower C contents used in current pipe steels, transformation to a fully martensitic microstructure is unlikely unless very low heat inputs are used or the steel has a high substititional alloy content; the HAZ CGHAZ microstructure is then more likely to consist of ferritic structures variously, termed 'carbide-free' bainite, quasi-polygonal ferrite, acicular or 'massive' ferrite [28], compare Figures 13 and 14. Such structures have inherently improved toughness on account of the higher transformation temperatures allowing some recovery of the dislocation sub-structure within the ferrite. If Si contents are much above 0.3-0.5% small islands of retained austenite may be present adding to toughness. Ni may also act in this way, but only if added in amounts above ~1%. There is a potential dilemma here because other work, mainly on TMCP plate steels, shows that the microstructure within the MA islands of retained phase also affects impact toughness and if partial transformation to martensite or bainite occurs toughness deteriorates. This is most likely to occur at high heat input which favours transformation temperatures over which such 'bainitic' HAZ structures evolve.
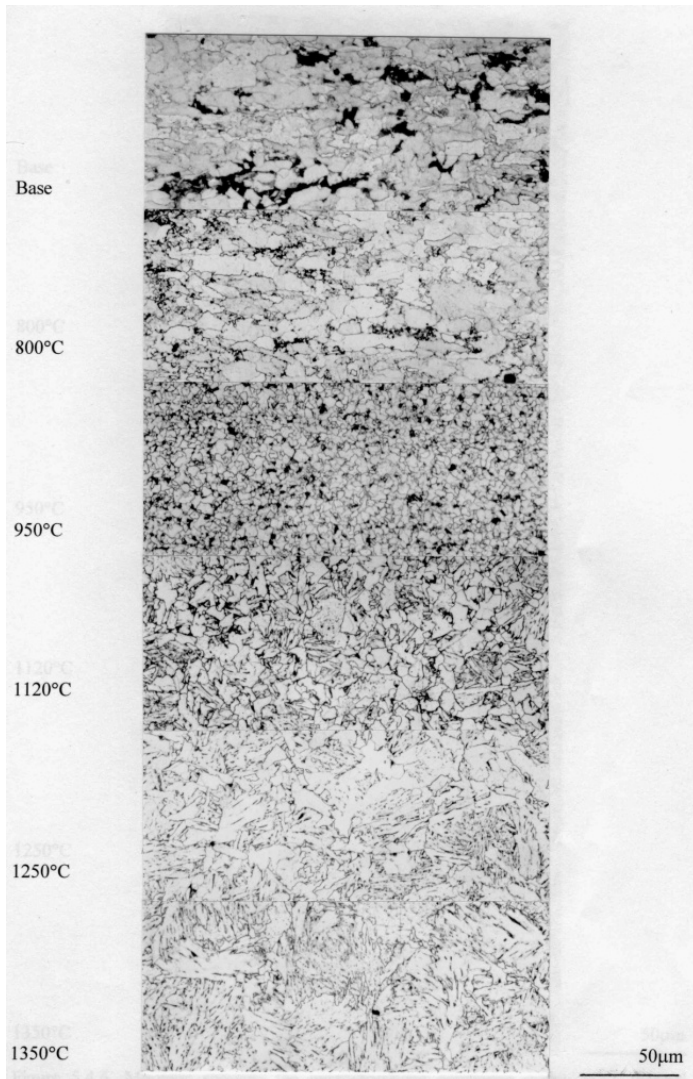
Figure 13. Photo-montage of HAZ simulated microstructures in a 0.08%C 0.31%Si 1.45%Mn
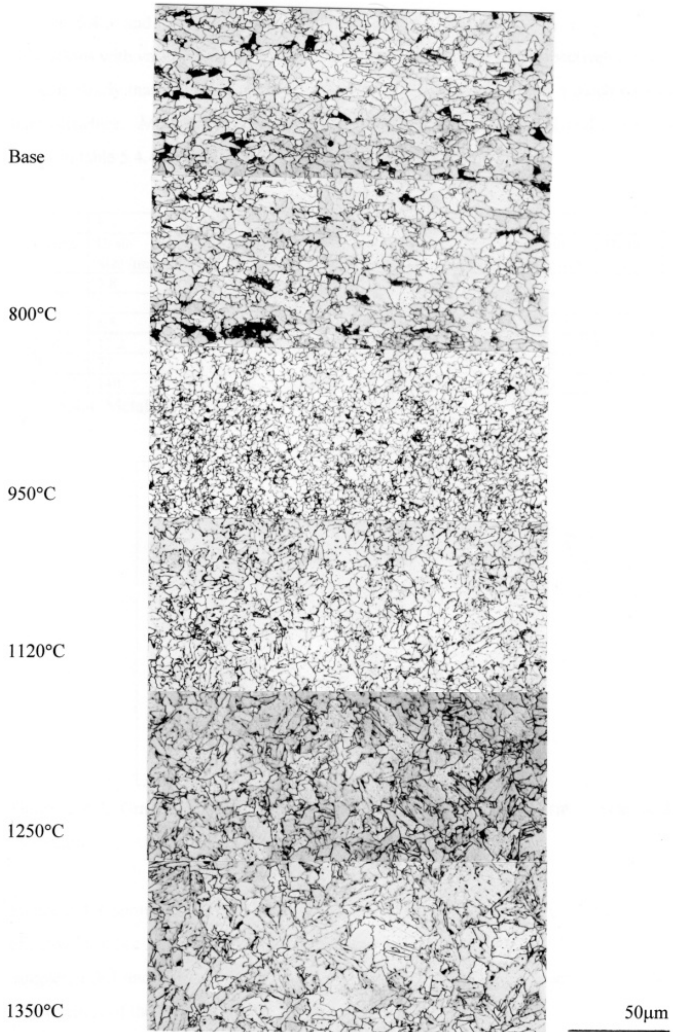0.036%Nb 0.057%V steel, peak temperatures are shown [72].

Figure 14. Photo-montage of HAZ simulated microstructures in a 0.048%C 0.32%Si 1.48%Mn 0.058%Nb 0.012%Ti steel, peak temperatures are shown [72].

Observations of crack paths in a very different microstructure common in weld metals, known as 'acicular' ferrite, AF, offer a possible solution to this dilemma. This microstructure consists of an interpenetrating array of ferrite laths with different variants of the Kurdjumov-Sachs relationship between austenite and ferrite. In this class of structure, crack deflection at the interlath boundaries is larger than for martensite and bainite because of the greater mis-orientation. The effective colony size (or fracture facet size) is, therefore, of the order of the lath size resulting in much superior toughness. This observation has also been invoked to interpret the improvements made to the base plate toughness of high strength pipe steels, X80 to X100, for Arctic service [29, 30]. Increasingly, this concept will find application to HAZ toughness provided that the acicular ferrite microstructure can be promoted in the HAZ by alloying. Many such attempts have been made ranging from the addition of stable oxide or sulphide particles, in an attempt to duplicate the effect found in weld metal where AF is nucleated by weld metal inclusions, to depressing the transformation temperature by alloying to promote AF formation [32-39]. The stable oxide approach is difficult to apply, primarily because solubilities are extremely low if Al deoxidation is used. Even if Al deoxidation can be avoided, by using Si or Ti for example [36, 37, 39], the volume fraction of oxides available is an order of magnitude smaller than that in weld metal so the effectiveness of the dispersion produced depends solely on the particle size achieved during solidification [37, 38]. These solidification rates are again one or two orders of magnitude slower than those of welds and this mitigates against obtaining an appropriate size range, ideally of the order of a few microns [36, 38]. On the other hand, doping with rare earth sulphides appears to be successful for some steel types; whether this technology can be applied to pipe compositions is uncertain [40].

To date, only V has been shown to have a direct influence on AF formation. The work of Edmonds [41] illustrates this but microstructures bearing the distinctive features associated with AF have been noted in the HAZ of more conventional steels containing both Nb and V [42, 43]. The mechanism is not understood but suggestions have been made regarding ferrite nucleation on pre-existing precipitates possibly those which are present from the processing and which have coarsened during the HAZ thermal cycle. One rather interesting observation comes from studies of laser welds in plate compositions not dissimilar to those used for pipe. These studies show that AF can be induced in autogenous (remelted plate) welds in low Al steels (typically less than 0.01%Al) by Ti additions [44]. The mechanism is obscure but may involve nucleation on complex oxide particles containing Ti (as in some weld metals) but other features of 'TiO' steels appear to suggest retardation of ferrite by Ti in solution which may also be important [45]. Other work has suggested ultra-low C steels with combinations of Nb and Ti together with C, Mo or B additions may promote these AF microstructures [46].

Turning to the effects of specific elements, in general, substitutional elements lower transformation temperature, raising hardness and lowering toughness. Exceptions to this are elements which stabilise austenite or show solid solution softening effects at high strain rates such as Si and Ni [47]. Currently, the level of Ni additions are such that any solid solution softening effect may have only a small influence on improving HAZ toughness. Silicon, on the other hand, can have a complex effect on toughness as it suppresses cementite formation. Consequently, during bainitic transformation, Si additions can prevent the formation of the inter-lath carbides and allow these carbon-rich regions to transform to a wide variety of microstructures at lower transformation temperatures. Depending on the cooling rate these regions can remain as austenite greatly improving toughness, alternatively, if they transform to martensite toughness dramatically deteriorates. Some indication of the potential differences

comes from studies of the effects of these carbon-rich regions, or M/A constituents, on ICCGHAZ toughness mainly on TMCP steels [48, 49]. For example, small amounts of M/A constituent are usually associated with CTOD transition temperatures below -30 $^{\circ}$C and are largely retained austenite at cooling times typical of welding at 5 kJ/mm. In contrast, large volume fractions of MA are often associated with high C brittle martensite with transition temperature above 25 $^{\circ}$C.

A feature of many modern pipe steels is the use of low P, S and N contents. The benefits of lowering the amounts of these elements are well recognised but are reaching the limits imposed by current steelmaking technology. The embrittlement by P is thought to be due largely to segregation to lath boundaries and may be exaggerated by sub-critical heat treatment [50, 51]. It was suggested that Mo or B additions could scavenge P reducing the potential for embrittlement by segregation. In this context it is interesting to note the use of these elements in recent high strength pipe steel developments [52, 53]. The rationale for reducing N content stems from the realisation that N in solid solution, 'free' N, is detrimental to toughness, for weld cooling times in the range 10 to 300 seconds; the change in impact transition temperature (ITT) is of the order of 25 $^{\circ}$C/0.001% 'free' N. Figure 15 shows the virtue of maintaining a high Al/N ratio although Ti additions would reduce 'free' N to a greater extent. Depending on the kinetics of dissolution (AlN in this case) the grain size of the CGHAZ could vary somewhat. The other issues raised by Ti additions to Nb steels are discussed below.
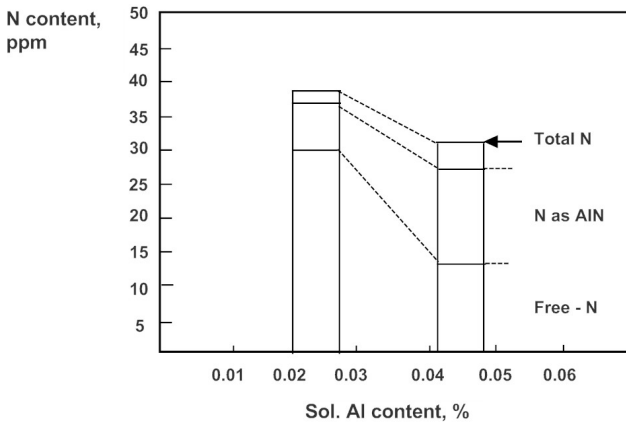

Figure 15. Illustrating the effect of Al content on soluble or 'free' N.

Effects of Microalloying

Effects on Microstructure and Toughness

As demonstrated by Kirkwood (these Proceedings) comparative exercises must be interpreted with caution and the apparent effect of niobium on CGHAZ toughness depends critically on, inter-alia composition and cooling rate. In this context, the results presented in Figure 16 should be interpreted carefully particularly as they are from thermal simulations rather than real welds. It should also be noted that the cooling times of primary interest are those below 100 secs, these being most representative of manual metal arc or submerged arc welding processes being employed on plate thicknesses relevant to linepipe welding.

At the 0.07% C level the results in Figure 16 suggest that with the particular analysis studied increasing niobium is not helpful to CGHAZ toughness and that an increase in carbon is, not surprisingly, very detrimental.
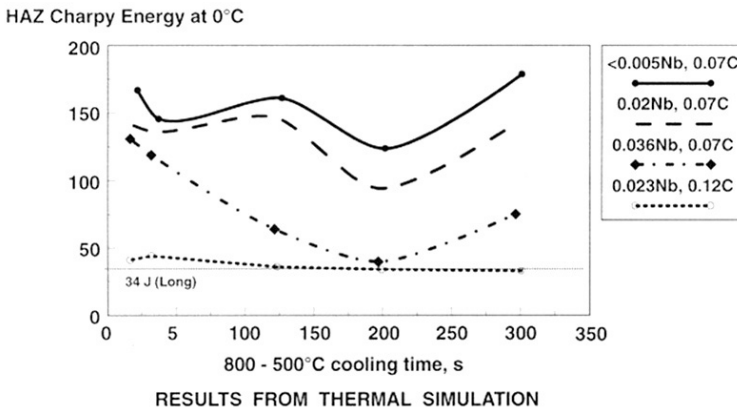
HAZ Charpy Energy at 0°C

Figure 16. Effect of C and Nb on simulated HAZ Charpy energy.

Further reductions in carbon content and/or decreases in Nb content alter this picture, both these changes leading to improvements. Such observations result from the balance between two competing influences of microalloying on the development of the HAZ microstructure. The first of these is due to the effects of microalloying on grain growth accompanying dissolution of the various compounds present after processing to pipe plate. The second is due to hardenability changes arising from the presence of microalloying elements redissolved during the HAZ thermal cycle. The relative effect on Ar3 is given in Figure 17 taken from studies by DeArdo [54] on TMCP steels, the data for 10 ^{o}C/s being relevant to HAZ conditions. The principal microalloying additions, Nb, V and Ti, are all ferrite stabilisers; the predicted rise in the equilibrium austenite to ferrite transformation temperature, Ae3 (Uhrenius) [55] can be significant but not easy to determine (Kirkaldy and Baganis) [56] unless near identical austenite grain size can be achieved. The temperatures at which the austenite to bainite transformation

174

takes place on cooling is also depressed by between 8 and 15 ^{o}C/0.01%Nb at typical pipe HAZ cooling rates.

This ability of niobium to depress transformation temperature arises because of its ability to suppress polygonal or Widmanstatten ferrite formation and may, in some circumstances, be used to advantage by reducing C content of the steel provided that the steel specification can still be met by, say, adjusting the post rolling cooling conditions. Excessive alloying using other conventional elements such as manganese, nickel etc. can, therefore, usually be avoided.

Several studies have confirmed Nb steels have a greater tendency to form bainite, indicated by a shift in the CCT diagram to longer times although direct comparisons are difficult because of differences in overall steel composition and austenite grain size. For example, the effect of increasing the reheating temperature from 1150 to 1250 ^{o}C is to decrease the cooling rate needed to form ferrite by about a factor of 2, ~11 ^{o}C/sec to ~7 ^{o}C/sec [57]. This contrasts with a steel of a similar C content but lower Mn which shows no ferrite forms in this range of cooling rate despite a lower austenitising temperature and finer grain size, 65μm [52]. These discrepancies are not easily explained but the comments made on precipitation sequences in complex microalloyed steels, [58-60] in the following section may be relevant.
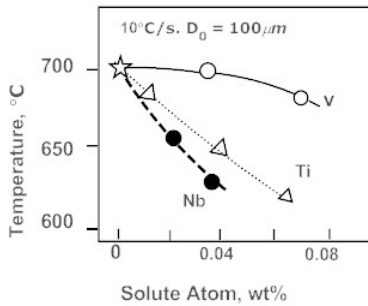

Figure 17. Effect of microalloying additions on austenite to ferrite transformation temperature.

Particle Dissolution, Composition and Grain Coarsening Response

The issue of particle dissolution and the resulting effect on HAZ grain size is more complex but has been modelled extensively and is widely accessible in the literature. While several of these models [61, 62] have been validated for commercial steels, there are some assumptions inherent in their use which should be tested further experimentally. The first assumption is that the particle size and distribution is assumed to be unimodal, uniformly distributed and their dissolution controls the resulting HAZ grain size. Given the sensitivity of the grain growth equations, such as those due to Gladman [63] or Hellman and Hillert [64], to particle size and volume fraction, the final HAZ grain size is likely to be quite dependent on details of the particle size distribution and the thermal cycle involved. The implication is that the presence of sufficient particles in the larger size classes, which would be the last to redissolve, should influence the

final HAZ austenite grain size. One clear consequence of this validates the use of higher Nb contents given that more and larger particles will be present as a consequence of the changed solubility throughout the processing; these will re-dissolve at substantially different rates to those in lower Nb steels delaying the onset of HAZ grain coarsening. A further point to note is that the particle size and distribution in TMCP steels will vary significantly with processing history, such as slab reheat temperature, rolling speed or reduction per pass during the final stages of rolling where much of the austenite conditioning so necessary for ferrite grain size control takes place. It should not be surprising therefore to find cases where near identical steel compositions which are produced on different mills differ appreciably in HAZ response. In addition, it would be of great interest to modify and then compare the predictions of current models for HAZ grain growth for cases where a bi- or tri-modal particle distribution is present as is the case for many TMCP rolling schedules.

The thermodynamic stability of the particles predicted from equilibrium models [65, 66] is also important in controlling grain growth which can be inhibited if the particles remain undissolved, for example in Nb/Ti or Ti treated steels, at the peak temperatures prevailing in the HAZ adjacent to the fused zone. Figure 18 shows some typical grain growth data showing that even residual levels of Ti, below ~0.007% depending on the source of the iron ores used in steelmaking, have an effect. These results may help interpret the appreciable scatter in austenite grain size for apparently similar steels subjected to the same weld thermal cycle.
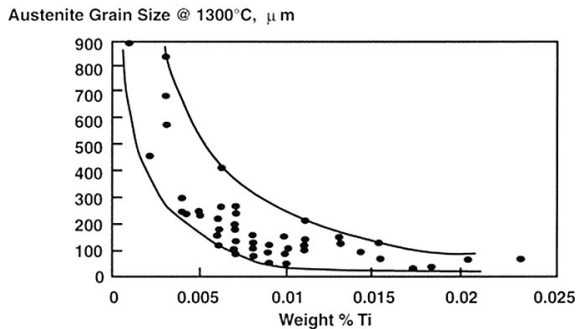

Figure 18. Results of HAZ grain coarsening experiments on steels illustrating the effects of Ti. Below ~0.01%, Ti is present as a residual element, above this represents a deliberate addition.

There is now considerable evidence from a large number of studies that the microalloying particle distribution is complex in terms of both particle size and composition, particularly if multiple microalloying elements are present. A typical case is Nb-Ti microalloyed steels, here the purpose of the Ti additions is to inhibit grain growth because TiN is virtually insoluble in austenite and therefore if the particle size is appropriate little or no HAZ grain growth results. However, the early simplistic idea that TiN and Nb(CN) precipitate as separate species was found to be incorrect, moreover, the particles were assumed to be homogeneous and single

phase. Due to the mutual intersolubility of all of the microalloy carbides or nitrides, particle compositions in the original plate microstructure are now known to vary considerably, although the details of the link with process history has not yet been clarified. Whilst the precipitation sequence can be predicted from equilibrium thermodynamics and many proprietary software packages (Thermocalc, Chemsage, MTdata) are available to estimate relative particle volume fractions and composition for a given steel composition, it is not clear to what extent these models accurately reflect actual particle composition for a particular process route and steel composition. However, it is known that there can be considerable deviation from equilibrium due to microsegregation in the cast steel [67] leading to complex precipitate morphologies before reheating [68, 69]. Such precipitate morphologies are broken down during slab reheating but enough microsegregation can remain leading to heterogeneity in austenite grain growth from point to point in the product [67]. Furthermore, given the limited diffusivity of substitutional alloying elements it is unreasonable to suppose this microsegregation would not be reflected in quite variable grain growth responses. Taking the diffusivity of Nb, Ti or V to be no greater than the self diffusivity of Fe (for 1350 ^{o}C these range from 7.85 x 10^{-14} for V to 4.3 x 10^{-13} for Nb [70, 71]) then under HAZ conditions the diffusion distances are only of the order of some 100s of nanometers compared to the CGHAZ grain size of the order of 100 μm. This observation then makes sense of the recurrent observations of 'caps' surrounding TiN particles in the HAZ, [59, 72]. An example is shown in Figure 19 [73]. The interpretation is that during the dissolution phase in the HAZ some of the Nb redissolves and is re-precipitated by heterogeneous nucleation on the undissolved $Ti_x(Nb)_yN$ during cooling. The net result is effectively to remove Nb from solution reducing both the hardenability of the HAZ austenite and the extent of precipitation strengthening possible during cooling. It might reasonably be inferred there may be circumstances where processing history impacts on the HAZ microstructure and mechanical properties.

a) EELS bright field image   b) EELS Ti map

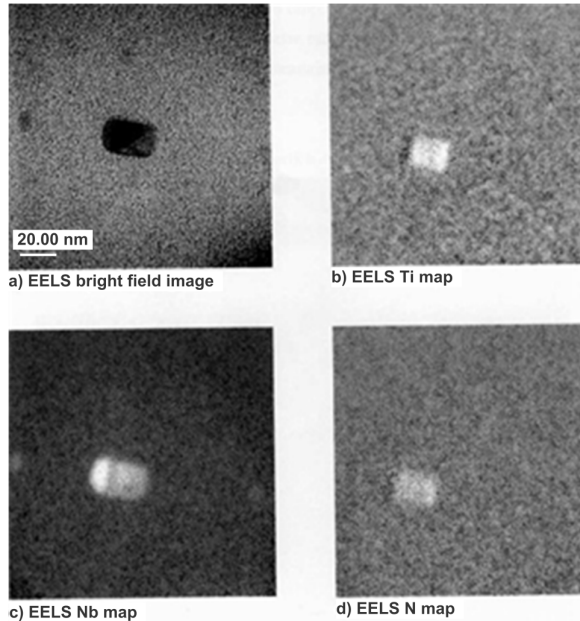c) EELS Nb map   d) EELS N map

Figure 19. Electron energy loss images of a 'capped' TiNbN in the HAZ of a 0.04%C 1.4%Mn 0.036%Nb steel. The lower left image shows the Nb 'cap', [72]

An Example of the Effect of Process Changes on HAZ Mechanical Properties and Microstructure.

The effects of process history on HAZ properties might well be obscured by differences in steel compositions or the sensitivity of pipe test results to notch location or testing regime. For example, thin wall, 8-10 mm, pipe can be produced via a coiled plate mill route or the reversing plate mill route. Yet, to generate equivalent properties different steel compositions would be used, obscuring any differences in HAZ toughness resulting from the different particle size distributions. Even with a single process route, say reversing plate mill, the range of process variables, for example, finish rolling or end hold temperatures, are generally small and with conventional specification testing regimes it would be extremely unlikely that significant changes in HAZ behaviour would be detected. Nevertheless, HAZ simulation of plates selected from extremes of normal production tolerances proved instructive, particularly where related to individual contributions to structure/property relationships. By selecting plates from a X65 pipe plate order produced to a nominal composition of 0.08%C 0.3%Si 1.45%Mn 0.042%Nb 0.06%V, the effect of extremes of finish rolling temperature and end hold temperature (EHT)

were examined using the Gleeble HAZ simulator [72]. The contributions to yield strength from precipitation and dislocation strengthening, σ_{p+d}, were found to track the range in EHT found in production. The extremes of the range were found to be 130 to 193 MPa and 760 to 816 $^\circ$C respectively with corresponding differences in impact behaviour, averages of 182 J compared with 93 J at the specified test temperature of -40 $^\circ$C. The particle size distributions were consistent with the estimated σ_{p+d} strengthening contribution. Small but significant differences in HAZ impact toughness were found after Gleeble simulation, 20 to 41 J at -20 $^\circ$C for the steel with the higher strengthening contribution compared to 114 to 148 J for the lower. In contrast, no such differences were found for a 0.045%C 0.3%Si 1.55%Mn 0.06%Nb 0.012%Ti steel processing via a coiled plate mill route despite appreciable differences in the σ_{p+d} contribution, 128 to 200 MPa, in this case, consistent with the reduced C content and reduced HAZ grain growth control by 'TiN', see Figure 14. Although there were no indications that the processing differences correlated with the limited routine HAZ toughness testing (one pipe per cast) required by the specification for the reasons already remarked on, some follow-up work was initiated. This made use of laboratory casts rolled to a variety of schedules designed to emphasise aspects of processing, particularly the rolling pass sequence during which Nb(CN) is precipitated in austenite [72,74]. A crude simulation of coiled plate production was made by hot charging plates into a furnace at 600 $^\circ$C and holding for 24 hours. A comparison of the Nb particle size distribution is shown in Figure 20, the differences due to processing are readily apparent. The σ_{p+d} contributions in the AR Nb, CR2 and CC conditions (see figure caption for these conditions, and the steel composition was 0.04%C 0.31%Si 1.4%Mn 0.036%Nb 0.04%Al 0.006%N) were 79, 136 and 0 MPa respectively and, as shown in Figure 21a, the corresponding CGHAZ ITT were -40, -27 and -44 $^\circ$C, but more importantly AR impact properties did not change after CGHAZ simulation. In contrast, the same rolling sequences applied to a Ti treated steel (as above but nil Nb 0.019%Ti 0.006%N) show much less variation in HAZ behaviour while suggesting a modest improvement to CGHAZ ITT in the AR condition, -65 compared to -60 $^\circ$C, Figure 21b. The extent to which these results mirror those from a 'real' HAZ on steels processed in this way is difficult to judge, but if the ICHAZ (950 and 1050 $^\circ$C simulation data) and CGHAZ simulation results are 'averaged' the CR2 condition would show behaviour closer to the parent steel, whereas the 'average' for the AR condition is dramatically improved. These differences are more or less in line with practical experience. Nevertheless, while showing only modest changes to HAZ behaviour these results demonstrate that processing can influence microstructural development during the weld thermal cycle and point to the critical nature of the CGHAZ in creating 'a local brittle zone'. The significance of this has been endlessly debated elsewhere!
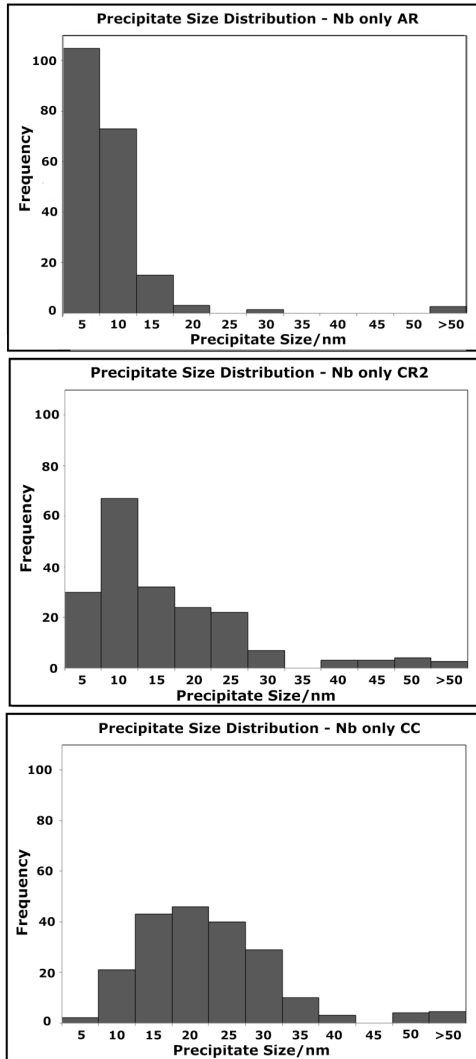
Figure 20. Particle size distribution for 3 different process routes: AR rolled rapidly to finish at ~1100 °C, CR2 rolled with holds in the range 1000-850 °C finishing at ~800 °C, CC as CR2 but hot charged into a furnace at 600 °C and cooled over 24 hours.
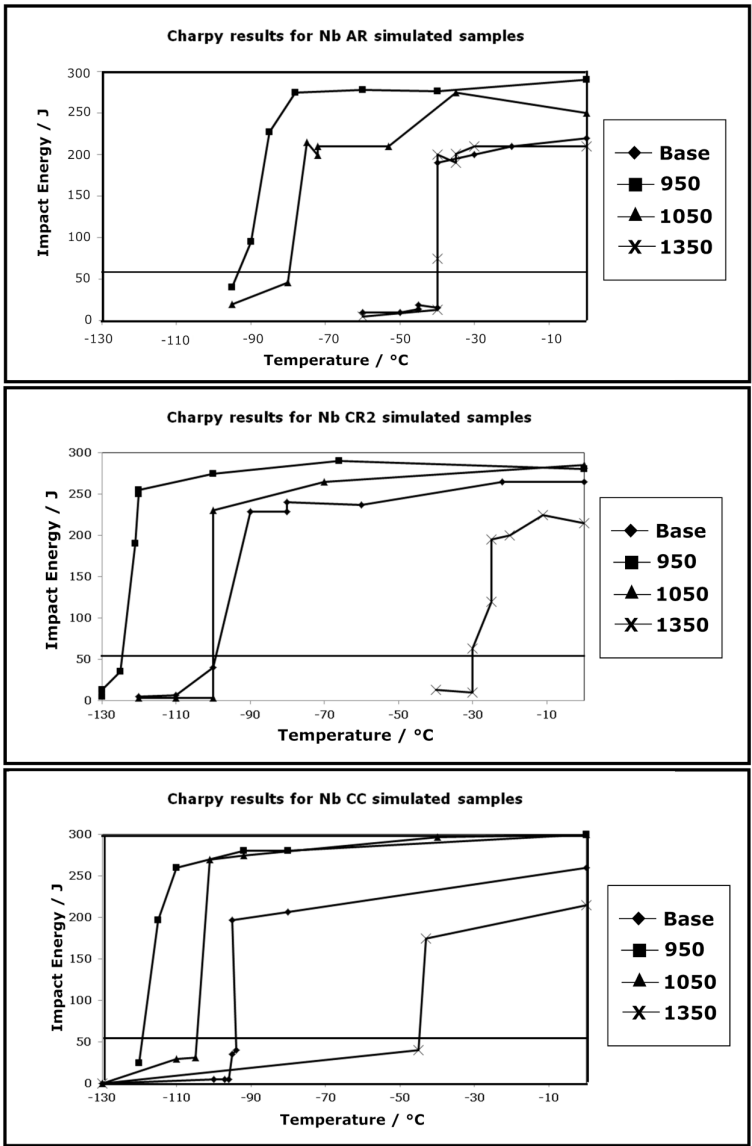
Figure 21a. HAZ Charpy energy data for the Nb steel in the AR, CR2 and CC conditions.
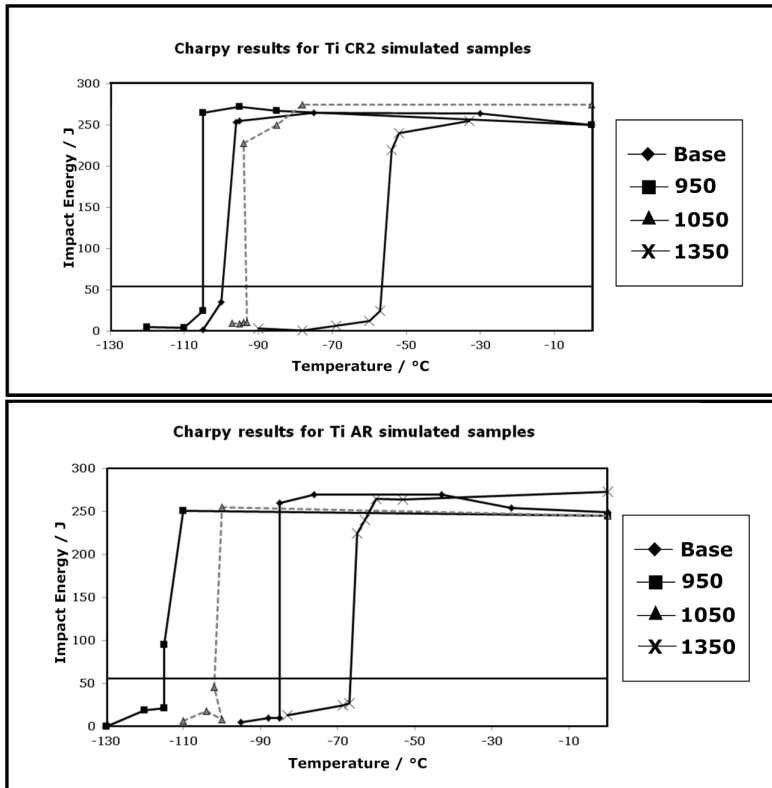
Figure 21b. HAZ Charpy energy data for the Ti steel after CR2 and CC processing.

The properties of modern pipe steels are heavily dependent on both chemistry and processing (rolling and cooling) regimes and in the quest to optimise parent plate properties and the response of the materials to welding, account must be taken of the way in which different distributions of precipitates may influence the development of microstructure in the heat affected zone. Results presented earlier demonstrate the potential sensitivity of certain steels to this phenomenon which may in some circumstances prove to be of practical relevance to welding engineers seeking to meet the most demanding requirements of recent specifications. In view of the sensitivity of some regions of the HAZ to changes in particle distribution and the dependence of such distributions on details of processing, in particular, the response of the microsegregated regions to heat treatment and subsequent effects on particle size and composition, it is the author's opinion that processing probably influences the HAZ response of pipe steels to a greater extent than realised.

Closing Comments

Reviewing the effects of pipe steel composition on the HAZ microstructure of seam welds, it might be concluded that current trends to reduce C content, increase the microalloying content, uniquely Nb, have greatly improved the weld HAZ toughness overall and that of the CGHAZ in particular. However, the rather poor properties of the IC and GRHAZ (and ICCGHAZ), albeit over a much narrower zone in the HAZ, remain and could be exacerbated by the increased alloying currently used for premium grade linepipe. Nevertheless there is the intriguing possibility that CGHAZ microstructures can be produced that lead to the possibility that there can be steels where no deterioration takes place after welding. This 'metallurgist's delight', would be complete, if in addition, the possibility of forming an HAZ consisting of acicular ferrite was realised by offering in excess of 600 MPa yield strength coupled with impact transition temperatures below -120 $^{\circ}$C (as in some seam welds but matching the parent plate properties of X80!!). Some combination of alloying with Nb and V might be found where NbCN particles remain in the HAZ for a sufficient time that they can influence HAZ grain coarsening, as already appears to be the case, and act as nucleation sites for ultra-fine ferrite grains, 1 to 3μm, during cooling, by both depressing transformation temperature [75] and altering the ferrite (or bainite) transformation mechanism. The role of V or Ti may also prove to be critical, as both of these elements have been implicated in the only proven cases where AF is found in amounts sufficient to alter the hardness/toughness balance in the CGHAZ. A case has also been made that process history influences the response of particular types of TMCP steels used for pipe applications.

References

1. D. Rosenthal, "The Theory of Moving Sources of Heat and its Application to Metal Treatments," *Transactions of the American Society of Mechanical Engineers*, 68 (1946), 819-866.

2. N. Yurioka, et al., "Welding Note," Nippon Steel Corporation, 1984.

3. P.L. Mangonon and M.A. Mahimkar, "Advances in Welding Science and Technology," *Proceedings of the 1st International Conference on Trends in Welding Research*, *TWR '86*, Gatlinburg, TN, ASM International, Metals Park, OH, (1986), 33–45.

4. B.A.Graville, "Cold Cracking in Welds in HSLA Steels," *Welding of HSLA (Microalloyed) Steels*, (1976), 85-101.

5. S. Hasebe, Y. Kawaguchi and Y. Arimochi, *The Sumitomo Search*, 11 (1) (1974), 1-24.

6. K. Lorenz and C. Duren, "C-Equivalent for Large Diameter Pipe Steels," *Proceedings of the Conference, Steels for Pipelines and Pipe Fittings,* London, (1981), paper 37.

7. T. Terasaki, T. Akiyama and M. Serino, "Chemical Composition and Welding Procedure to avoid Hydrogen Cold Cracking," *Proceedings of the International Conference. Joining of Metals*, Helsingfors, Denmark, (1984), 381-386.

8. H. Suzuki, "A New Formula for Estimating HAZ Hardness in Welded Steels," IIW Doc. IX-1315-85, (1985).

9. N. Yurioka et al., "Prediction of HAZ Hardness of Transformable Steels," *Metal Construction,* 19 (4) (1987), 217.

10. Y. Ito and K. Bessyo, "Weldability Formula of High Strength Steels Related to HAZ Cracking," IIW Doc. IX-567-68 (1968).

11. R.C. Cochrane, British Steel unpublished studies of grain growth in HSLA steels (1981-1986).

12. S. Sekino and N. Mori, *Proceedings of the International Steel Institute of Japan* (supplement) 11 (1971), 1181-1183.

13. R.A. Grange, "Effect of Microstructural Banding in Steel," *Metallurgical Transactions,* 2 (1) (1971), 65-78.

14. R.C. Cochrane and W.B. Morrison, unpublished work, British Steel Corporation.

15. M. Nakanishi, Y. Komizo and Y. Fukada, "Study on the Critical CTOD Properties in the Heat Affected Zone of C-Mn Micro Alloyed Steel," *The Sumitomo Search*, 33 (2) (1986), 22-34.

16. P. Maynier, J. Dollet and P. Bastien, "Prediction of Microstructure via Empirical Formulas Based on CCT Diagrams," *Proceedings of the International Conference. Hardenability Concepts with Applications to Steel*, Warrendale, PA, The Metallurgical Society of AIME, (1978), 163-178.

17. L. Devilliers, D. Kaplan and P. Testard, "Predicting the Microstructures and Toughness of Weld HAZs," *Welding International*, 9 (2) (1995), 128-138.

18. S. Denis, D. Farias and A. Simon, "Mathematical Model Coupling Phase Transformations and Temperature Evolutions in Steels," *Iron and Steel Institute of Japan.* 32 (3) (1992), 316-325.

19. G.K. Adil and S.D. Bhole, "HAZ Hardness and Microstructure Predictions of Arc Welded Steels, I. Review of Predictive Models," *Canadian Metallurgical Quarterly*, 31 (2) (1992), 151-157.

20. P.R. Kirkwood, "A Viewpoint on the Weldability of Modern Structural Steels," *Proceedings of the International Symposium, Welding Metallurgy of Structural Steels*, Denver, Colorado, USA, (1987), 21-45.

21. P.H.M. Hart, *Proceedings of the International Conference Metallurgical and Welding Advances in High Strength Low Alloy Steels*, Copenhagen, (September 1984).

22. P.L. Harrison and P.H.M. Hart, *Proceedings of the International Conference, Microalloying*, Houston, Texas, USA, (1990), 604-637.

23. Y. Yurioka, "TMCP Steels and their Welding," *Welding in the World*, 35 (6) (1995), 375s-390s.

24. Y. Tomita and K. Okabayashi, "Effect of Microstructure on Strength and Toughness of Heat-Treated Low Alloy Structural Steels," *Metallurgical Transactions,* 17A (7) (1986), 1203-1209.

25. J.P. Naylor, "The Influence of Lath Morphology on the Yield Stress and Transition Temperature of Martensitic-Bainitic Steels," *Metallurgical Transactions,* 10A (7) (1979), 861-873.

26. P. Brozzo, G. Buzzichelli, A. Mascanzoni and M. Mirabile, "Microstructure and Cleavage Resistance of Low-C Bainitic Steels," *Metal Science,* 11, (1977), 123-129.

27. R.C. Cochrane, British Steel/Nippon Steel Technical Exchange Report 1984.

28. S.W. Thompson, D.J. Colwyn and G. Krauss, "Continuous Cooling Transformations and Microstructures in a Low-Carbon, High-Strength Low-Alloy Plate Steel," *Metallurgical Transaction*, 21A (6) (1990), 1493-1507.

29. W. Wang, Y. Shan and K. Yang, *Materials Science and Engineering*, A502 (2008), 38-44.

30. A. Guo et al., "Ultrahigh Strength and Low Yield Ratio of Niobium- Microalloyed 900 MPa Pipeline Steel with Nano/Ultrafine Bainitic Lath," *Materials Science and Technology,* A527 (2010), 3886-3892.

31. A.R. Mills, G. Thewlis and J.A. Whiteman, "Nature of Inclusions in Steel Weld Metals and their Influence on Formation of Acicular Ferrite," *Materials Science and Technology,* 3 (12) (1987), 1051-1061.

32. M.N. Ilman, "The Development of Acicular Ferrite in C-Mn Steel Weld Metals Containing Titanium, Boron, Aluminium and Nitrogen" (Ph.D. thesis, University of Leeds, 2001) and M.N. Ilman and R.C.Cochrane, to be published, IIW Conference, May 2010.

33. Ø. Grong, et al., "Catalyst Effects in Heterogeneous Nucleation of Acicular Ferrite," *Metallurgical and Materials Transactions A*, 26 (3) (1995), 525-534.

34. F.J. Barbaro, P. Krauklis, and K.E. Easterling, "Formation of Acicular Ferrite at Oxide Particles in Steels," *Materials Science and Technology*, 5 (11) (1989), 1057-1068.

35. J.H. Shim et al., "Nucleation of Intragranular Ferrite at Ti_2O_3 Particle in Low Carbon Steel, *Acta Materialia*, 47 (9) (1999), 2751-2760.

36. Y. Tomita et al., "Improvement in HAZ Toughness of Steel by TiN-MnS Addition," *The Iron and Steel Institute of Japan International,* 34 (10) (1994), 829-835.

37. T.K. Lee et al., "Effect of Inclusion Size on the Nucleation of Acicular Ferrite in Welds," *The Iron and Steel Institute of Japan International,* 40 (12) (2000), 1260-1268.

38. Y.T. Pan and J.L. Lee, "Development of TiO_x-Bearing Steels with Superior Heat-Affected Zone Toughness," *Materials and Design*, 15 (6) (1994), 331-338.

39. S. Ohkita et al., "Improvement of HAZ Toughness of High Strength Low Alloy Steel by Finely Dispersed Titanium Oxide," *Nippon Steel Technical Report* 37, (April 1988), 10-16.

40. G. Thewlis, "Effect of Cerium Sulphide Particle Dispersions on Acicular Ferrite Microstructure Development in Steels," *Materials Science and Technology*, 22 (2) (2006), 153-166.

41. K. He and D.V. Edmonds, "Formation of Acicular Ferrite and Influence of Vanadium Alloying," *Materials Science and Technology,* 18 (3) (2002), 289-296.

42. P.H.M. Hart and P.S. Mitchell, "The Effect of Vanadium on the Toughness of Welds in Structural and Pipeline Steels," *Welding Journal,* 74 (7) (1995), 239s-248s.

43. R. Otterberg, R. Sandström and A. Sandberg, "Influence of Widmanstätten Ferrite on Mechanical Properties of Microalloyed Steels," *Metals Technology*, 7 (1) (1980), 397-408.

44. R.C. Cochrane and D.J. Senogles, *Proceedings of Conference Titanium Technology in Microalloyed Steels*, ed. T.N. Baker (Sheffield, Institute of Materials, 1995).

45. H.I. Jun et al., *Materials Science and Engineering,* 427 (A) (2006), 157-162.

46. M.F. Eldridge, "The Transformation Behaviour of Low Aluminium Ferritic Steels" (Ph.D. thesis, University of Leeds, 2000).

47. W.C. Leslie, "Iron and its Dilute Substitutional Solid Solutions," *Metallurgical Transactions,* 3 (1) (1971), 5-26.

48. J.H. Chen et al., "Micro-Fracture Behaviour Induced by M-A Constituent (Island Martensite) in Simulated Welding Heat Affected Zone of HT80 High Strength Low Alloyed Steel," *Acta Metallurgica,* 32 (10) (1984), 1779-1788.

49. R. Taillard et al., "Effect of Silicon on CGHAZ Toughness and Microstructure of Microalloyed Steels," *Metallurgical and Materials Transactions* A, 26 (2) (1995), 447-457.

50. R.G. Faulkner, "Influence of Phosphorus on Weld Heat Affected Zone Toughness in Niobium Microalloyed Steels", *Materials Science and Technology*, 5 (11) (1989), 1095-1101.

51. C. Thaulow, A. Paauw and K. Guttermsen, "The Heat Affected Toughness of Low-Carbon Microalloyed Steels," *Welding Journal,* 66 (9) (1987), 226s-279s.

52. Y.B. Xu et al., "Microstructural Evolution in an Ultra Low-C and High-Nb Bearing Steel during Continuous Cooling," *Materials Science,* 44 (2009), 3928–3935.

53. Y.M. Kim, H. Lee and N.J. Kim, "Transformation Behavior and Microstructural Characteristics of Acicular Ferrite in Linepipe Steels," *Materials Science and Engineering,* 478 (A) (2008), 361-370.

54. A.J. DeArdo, "Niobium in Modern Steels," *International Materials Review,* 48 (6) (2003), 371-408.

55. Bjorn Uhrenius, *Hardenability Concepts with Applications to Steel*, ed. V. Doane and J.S. Kirkaldy, (The Metallurgical Society of the American Institute of Mining, Metallurgical and Petroleum Engineers, 1978), 28-81.

56. J.S. Kirkaldy, and E.A. Baganis, "Thermodynamic Prediction of the Ae3 Temperature of Steels with Additions of Mn, Si, Ni, Cr, Mo, Cu.," *Metallurgical Transactions* A, 9 (4) (1978), 495-501.

57. K. Hulka, J.M. Gray and K. Heisterkamp, "Metallurgical Concept and Full Scale Testing of a High Toughness, H2S Resistant 0.03 % C - 0.10 % Nb Steel" (Niobium Technical Report NbTR-16/90 CBMM Brazil, 1990).

58. D.C. Houghton, G.C. Weatherly and J.D. Embury, "Thermomechanical Processing of Austenite," Pittsburgh, USA, 1981, (American Institute of Mining, Metallurgical and Petroleum Engineers, 1982), 267.

59. D.C Houghton. *Acta Metallurgica,* 41 (10) (1993), 2293-3006.

60. J.T. Bowker, J. Ng-Yelim and T.F. Malis, "Effect of Weld Thermal on Behaviour of Ti-Nb Carbonitrides in High Strength Low Alloy Steel," *Materials Science and Technology,* 5 (10) (1989), 1034-1036.

61. M. Hillert and L. I. Staffansson, L. I. "Regular-Solution Model for Stoichiometric Phases and Ionic Melts," *Acta Chemica Scandinavica,* 24 (10) (1970), 3618-3626.

62. H. Adrian, *Materials Science and Technology,* 8, (1992), 406-419.

63. T. Gladman, "On the Theory of the Effect of Precipitate Particles on Grain Growth in Metals," *Proceedings of the Royal Society of London, Series A, Mathematical and Physical Sciences*, 294 (1438) (1966), 298-309.

64. P. Hellman and M. Hillert, "Effect of Second-Phase Particles on Grain Growth," *Scandinavian Journal of Metallurgy,* 4 (5) (1975), 211-219.

65. I. Anderson, O. Grong and N. Fyum, *Acta Metallurgica et Materialia*, Parts I and II, 43 (7) (1995), 2673-2700.

66. J.C. Ion, K.E. Easterling and M.F. Ashby, "A Second Report on Diagrams of Microstructure and Hardness for Heat-Affected Zones in Welds," *Acta Metallurgica*, 32 (11) (1984), 1949-1962.

67. A.J. Couch, "Grain Growth and Dissolution Kinetics in High Strength Low Alloy (HSLA) Steels," (Ph.D thesis, University of Leeds, 2001).

68. J.M. Raison, (M.Sc thesis, University of Birmingham, 1982).

69. Z. Chen, M.H. Loretto, and R.C. Cochrane, "Nature of Large Precipitates in Titanium-Containing High Strength Low Alloy Steels," *Materials Science and Technology,* 3 (10) (1987), 836-844.

70. A.W. Bowen, and G. Leak, "Diffusion in Bcc Iron Base Alloys," *Metallurgical Transactions,* 1 (10) (1970), 2767-2773.

71. E.A. Brandes, and C.J. Smithells, *Metals Reference Handbook* (London, UK: Butterworths, 1983).

72. D.J. Egner, "The Effect of Thermomechanical Processing on the Heat Affected Zone Formation of Microalloyed Steels" (Ph.D. thesis, University of Leeds, 1999).

73. D.J. Egner and R.C. Cochrane, "Process History, Microstructure and Weldability Interactions in Microalloyed Steels," *Materials Science Forum*, 284-286 (1998), 279-286.

74. D.J. Egner, R.C. Cochrane, and R. Brydson, "Dissolution Behaviour of Precipitates in the HAZ of Microalloyed Steels," *Proceedings of Institute of Physics Conference, The Electron Microscopy and Analysis Group (EMAG),* (1999) see also [72] 189-192.

75. R.C. Cochrane and W.B. Morrison, "Transformation Characteristics of Some Linepipe Steels Containing Nb, V and Mo and Their Relationship to Processing and Microstructure," *Proceedings of the International Conference Steels for Linepipe and Pipeline Fittings* (London, UK: The Metals Society, 1981), paper 7.

Acknowledgements